Exploring the limits of the Jenkinson–Collison weather types classification scheme: a global assessment based on various reanalyses

Juan A. Fernández-Granja[1] · Swen Brands[2] · Joaquín Bedia[3,4] · Ana Casanueva[3,4] · Jesús Fernández[1]

Abstract

The Jenkinson–Collison weather typing scheme (JC-WT) is an automated method used to classify regional sea-level pressure into a reduced number of typical recurrent patterns. Originally developed for the British Isles in the early 1970's on the basis of expert knowledge, the method since then has seen many applications. Encouraged by the premise that the JC-WT approach can in principle be applied to any mid-to-high latitude region, the present study explores its global extra-tropical applicability, including the Southern Hemisphere. To this aim, JC-WT is applied at each grid-box of a global 2.5° regular grid excluding the inner tropics (± 5° band). Thereby, 6-hourly JC-WT catalogues are obtained for 5 distinct reanalyses, covering the period 1979–2005, which are then applied to explore (1) the limits of method applicability and (2) observational uncertainties inherent to the reanalysis datasets. Using evaluation criteria, such as the diversity of occurring circulation types and the frequency of unclassified situations, we extract empirically derived applicability thresholds which suggest that JC-WT can be generally used anywhere polewards of 23.5°, with some exceptions. Seasonal fluctuations compromise this finding along the equatorward limits of the domain. Furthermore, unreliable reanalysis sea-level pressure estimates in elevated areas with complex orography (such as the Tibetan Plateau, the Andes, Greenland and Antarctica) prevent the application of the method in these regions. In some other regions, the JC-WT classifications obtained from the distinct reanalyses substantially differ from each other, which may bring additional uncertainties when the method is used in model evaluation experiments.

Keywords Jenkinson–Collison classification · Weather types · Observational uncertainty · Transition probabilities

✉ Juan A. Fernández-Granja
  juan.fernandez@unican.es

  Swen Brands
  swen.brands@gmail.com

  Joaquín Bedia
  joaquin.bedia@unican.es

  Ana Casanueva
  ana.casanueva@unican.es

  Jesús Fernández
  jesus.fernandez@unican.es

1 Instituto de Física de Cantabria (IFCA), CSIC-Universidad de Cantabria, 39005 Santander, Spain

2 MeteoGalicia, Consellería de Medio Ambiente, Territorio y Vivienda, Xunta de Galicia, Santiago de Compostela, Spain

3 Dept. Matemática Aplicada y Ciencias de la Computación (MACC), Universidad de Cantabria, 39005 Santander, Spain

4 Grupo de Meteorología y Computación, Universidad de Cantabria, Unidad Asociada al CSIC, 39005 Santander, Spain

1 Introduction

Large-scale circulation patterns exert a direct influence on the regional climate. For instance, persistent high pressure (blocking) systems (Rex 1950; Jury et al. 2019) and the North Atlantic Oscillation (NAO) pattern (Hurrell et al. 2003; Folland et al. 2009) disturb the predominant cyclonic westerly flow (Sillmann and Croci-Maspoli 2009), which largely modulates the European climate. As a consequence, changes in seasonal extreme events occur, such as those related to high temperature (Buehler et al. 2011; Barriopedro et al. 2011; Favá et al. 2015; Schaller et al. 2018), wet spells and precipitation extremes (Busuioc et al. 2001; Casanueva et al. 2014; Sousa et al. 2017) or droughts (Bladé et al. 2011).

Similarly, in the South Hemisphere (SH), the Southern Annular Mode (SAM), also referred as the Antarctic Oscillation, influences the climate systems at high and middle latitudes (Gong and Wang 1998, 1999; Thompson and Wallace 2000; Thompson et al. 2000), displaying a 'seesaw' pattern for the atmospheric mass (sea-level pressure -SLP- or geopotential heights). In

essence, the SAM consists of a belt of strong westerly winds or low pressures surrounding Antarctica which exhibits a northward/southward displacement as its main mode of variability. For example, it is associated with storms and cold fronts that move from west to east largely determining precipitation in southern Australia (Stammerjohn et al. 2008; Risbey et al. 2009). Additionally, various modes of large-scale climate variability such as the El Niño-Southern Oscillation (ENSO), the Interdecadal Pacific Oscillation (IPO), the Indian Ocean Dipole (IOD), the Subtropical ridge (STR) or the Madden Julian Oscillation (MJO) largely determine the regional climate of the SH (Dey et al. 2019).

Hence, an adequate representation of atmospheric circulation and high/ low pressure variability becomes essential for a proper description of the main regional climate features. In this context, synoptic weather types are a useful tool as they summarize the whole range of variability of the data into a few, construable patterns (Huth et al. 1993, 2008; Littmann 2000; Stryhal and Huth 2017). A well-known circulation classification method is the Lamb Weather Type (LWT) Classification. The LWT classification is a subjective clustering approach created by the climatologist Hubert H. Lamb (Lamb 1972) with the aim of studying the synoptic climatology over the British Isles. The system relies on a deterministic weather type classification based on a number of rules requiring meteorological expert knowledge for the interpretation of daily SLP charts, providing a straightforward and well defined physical interpretation of the SLP patterns. Later in the computer era, Jenkinson and Collison (1977) developed a more objective scheme following Lamb's principles, known as the Jenkinson-Collison weather type classification (JC-WT hereafter). The JC-WT approach is an automated procedure using a set of equations based upon SLP able to reproduce circulation types with negligible differences from the original LWT catalogue (Jones et al. 1993). Furthermore, unlike the original LWT approach, the JC-WT scheme has the advantage of being automatically applicable to different geographical locations through the introduction of some adjustment parameters to account for the relative grid spacing as a function of latitude.

The advantages of this circulation typing method has since then been exploited in different studies in the Northern Hemisphere (NH). For instance, JC-WTs have been centered in the Iberian Peninsula [10°W, 40°N] (Trigo and DaCamara 2000), [5°W, 40°N] (Ramos et al. 2014), western Mediterranean basin [5°E, 40°N] (Grimalt-Gelabert et al. 2013), southern Scandinavia [15°E, 60°N] (Chen 2000), Central Europe [10°E, 50°N] (Donat et al. 2010), south-west Russia [55°E, 55°N] (Spellman 2017), Ireland [10°W, 55°N] (Fealy and Mills 2018), Serbia [20°E, 42.5°N] (Putnikovic et al. 2016) and southeastern China (Wang and Sun 2020; Wu et al. 2020). Otero et al. (2018) computed, for the first time, a spatially continuous application of the JC-WT classification over Europe [13°W − 34°E, 34°N − 71°N] and, in an unprecedented study, Brands (2022) computed JC-WTs on every grid-box covering the

majority of the NH extratropic region in order to evaluate GCM performance. The JC-WT classification has been seldom used in the southern hemisphere, excepting, to the best of our knowledge, by Sarricolea et al. (2018) in southern Chile [72.5°W, 42.5°S], requiring in this case an adaptation of the model equations to the SH circulation, as illustrated in this study.

The idea of evaluating model performance by means of weather types started long time ago (Jones et al. 1993; Hulme et al. 1993), and the process-based evaluation paradigm has recently come into focus particularly within the downscaling community (Maraun et al. 2017), primarily aimed in this case at performing an optimal, objective selection of GCMs for downscaling experiments (Pickler and Mölg 2021). The JC-WT classification, built upon SLP fields only, is somewhat limited in its ability to infer other atmospheric features related to atmospheric circulation in a broad context. However, important information regarding low level circulation physics can also be inferred from the analysis of the JC intermediate parameters, such as air flows and shear vorticities. The relatively easy interpretation of these airflow indices and the simplicity of the JC method, which allows transferability to other regions with a simple implementation, make it the preferred classification scheme in previous studies (e.g. Otero et al. 2018). Moreover, as shown by Conway and Jones (1998), circulation patterns fundamentally control meteorological characteristics on the surface, whereby the use of SLP has a lot of advantages. Quoting Sterl (2004), 'if the pressure fields of two models differ, most other fields will differ too', which highlights the importance of SLP as the basic dynamical variable of a model and its relevance for model assessment. In this sense, model performance can be assessed by relying on SLP-based classification techniques such as the JC-WT classification, as an effective tool for model ranking and selection (see e.g., Fernandez-Granja et al. 2021))

Model evaluation involves the analytical comparison of model outputs against observations (or reanalysis, as pseudo-observations), taking into account that not only the model, but also the observations may be uncertain (Gettelman and Rood 2016; Kotlarski et al. 2019. Most often, reanalysis products are used as reference, requiring a careful consideration of the divergence in their representation of climate features, particularly in regions where their background observational network has been historically sparse (Sterl 2004; Lavin-Gullon et al. 2021) and those more sensitive to temporal non-stationarities in the assimilated data incorporated to the model by the observing systems (Bengtsson 2004). As a result, it is widely recognized the need to consider multiple observational products when evaluating climate models (Gibson et al. 2019) and considerable effort has been devoted to the intercomparison of reanalysis products in different climate research contexts (e.g. Chen et al. 2008; Ben Daoud et al. 2009; Brands et al. 2012) and the understanding of the underlying causes for their disagreement (Fujiwara et al. 2017).

This study describes the implementation of the JC-WT classification for its application worldwide, including its adaptation

Table 1 Equations of the different circulation parameters of the JC-WT classification, for Northern and Southern Hemispheres

Param.	Northern hemisphere	Southern hemisphere	Wind-flow characteristics
W	$\dfrac{P_{12}+P_{13}}{2}-\dfrac{P_4+P_5}{2}$	$\dfrac{P_4+P_5}{2}-\dfrac{P_{12}+P_{13}}{2}$	Westerly flow
S	$s\left(\dfrac{P_5+2P_9+P_{13}}{4}-\dfrac{P_4+2P_8+P_{12}}{4}\right)$	$s\left(\dfrac{P_4+2P_8+P_{12}}{4}-\dfrac{P_5+2P_9+P_{13}}{4}\right)$	Southerly flow
D	$\arctan\dfrac{W}{S}$		Flow direction
F	$\sqrt{W^2+S^2}$		Resultant flow
Z_W	$z_w^-\left(\dfrac{P_{15}+P_{16}}{2}-\dfrac{P_8+P_9}{2}\right)$ $-z_w^+\left(\dfrac{P_8+P_9}{2}-\dfrac{P_1+P_2}{2}\right)$	$z_w^+\left(\dfrac{P_1+P_2}{2}-\dfrac{P_8+P_9}{2}\right)$ $-z_w^-\left(\dfrac{P_8+P_9}{2}-\dfrac{P_{15}+P_{16}}{2}\right)$	Westerly shear vorticity
Z_S	$z_s\left(\dfrac{P_6+2P_{10}+P_{14}}{4}-\dfrac{P_5+2P_9+P_{13}}{4}\right.$ $\left.-\dfrac{P_4+2P_8+P_{12}}{4}+\dfrac{P_3+2P_7+P_{11}}{4}\right)$	$z_s\left(\dfrac{P_3+2P_7+P_{11}}{4}-\dfrac{P_4+2P_8+P_{12}}{4}\right.$ $\left.-\dfrac{P_5+2P_9+P_{13}}{4}+\dfrac{P_6+2P_{10}+P_{14}}{4}\right)$	Southerly shear vorticity
Z	Z_W+Z_S		Total shear vorticity

where $s=\dfrac{1}{\cos\psi}$; $z_w^-=\dfrac{\sin\psi}{\sin(\psi-5°)}$; $z_w^+=\dfrac{\sin\psi}{\sin(\psi+5°)}$; $z_s=\dfrac{1}{2\cos^2\psi}$

Figure 1 displays the relative position of the points $i=1,\ldots,16$, where SLP values P_i are considered

to SH locations, and presents a 6-hourly database of JC-WT catalogues calculated from five different reanalysis products with a global coverage (excluding a 10°-width band along the equator). The objective of this work is two-fold. First, we undertake an assessment of the JC-WT applicability across the globe, taking as reference the latest IPCC-WGI Reference Regions (Iturbide et al. 2020) for summarizing the results. These allow for the identification of the global areas where the JC-WT classification provides an effective tool for characterizing the SLP patterns. Second, the different JC-WT reanalysis catalogues are compared with the aim of unveiling regions with high observational uncertainty. Caution is advocated in these areas, where the usage of more than one reanalysis is required in order to adequately evaluate the range of uncertainty in circulation-dependent modelling and/or downscaling exercises. The global JC-WT catalogues and the code implementing the worldwide JC-WT formulation used in this study are made available through dedicated Zenodo and GitHub open repositories.

2 Methodology and data

2.1 Jenkinson–Collinson classification

We follow the JC-WT formulation developed by Jenkinson and Collison (1977) that yields 27 different types. As input, we use 6-hourly, instantaneous sea-level pressure (SLP) data, which are

sampled using a cross-shaped point pattern (Fig. 1) formed by 16 points with a separation of 5° in latitude and 10° in longitude. Due to its shape, in the following, we will refer to this scheme simply as "cross". This cross can, in principle, be centered on any extra-tropical location.

The JC-WT classification is a function of 6 parameters related to wind-flow characteristics. Their corresponding equations are summarized in Table 1: southerly flow (S), westerly flow (W), total flow (F), southerly shear vorticity (Z_S), westerly shear vorticity (Z_W) and total shear vorticity (Z) computed upon the SLP records provided at a given time (6-hourly records in this study). The original parameter equations proposed by Jenkinson and
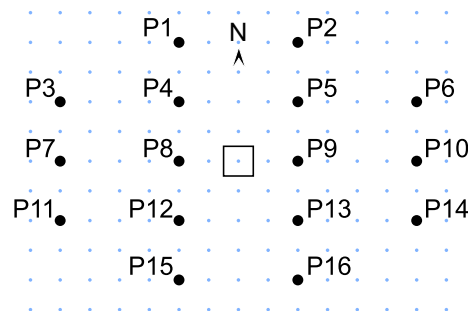
Fig. 1 Spatial distribution of the grid point pattern ("cross") of 16 points (in black) used in the JC-WT equations from Table 1. The background grid (in blue) represents the common, 2.5° regular grid, where the SLP has been interpolated. The square indicates the central grid cell of the cross, located at latitude ψ (see equations in Table 1)

Table 2 Set of reanalyses used in this study, their nominal resolution at the equator (in °) and modelling centers producing them

| Reanalysis	Nom. res. (°)	Modelling center	References
ERA-20C	1.13	ECMWF	Poli et al. (2016)
ERA-Interim	0.75	ECMWF	Dee et al. (2011)
ERA-5	0.25	ECMWF	Hersbach et al. (2020)
JRA-55	1.25	JMA	Kobayashi et al. (2015); Harada et al. (2016)
NCEP Reanalysis 1	2.5	NCEP-NCAR	Kalnay et al. (1996)

ECMWF European Center for Medium Range Weather Forecasts, *JMA* Japanese Meteorological Agency, *NCEP-NCAR* National Centers for Environmental Prediction/National Center for Atmospheric Research.

Collison (1977) require further adjustments for their application in SH locations (Table 1). The result is a set of 27 weather types representing pure cyclonic (C) and anticyclonic (A) circulation over the center point, 8 pure directional types (N, NE, E, ..., NW), 16 hybrid types (mixing A or C with any of the directional types) and a 27th type accounting for unclassified records, that is, days with chaotic weak flow or days when incompatible hybrids are formed (Fig. 2). Equations for S, Z_W and Z_S use a number of adjustment coefficients (s, z_w^-, z_w^+, z_s) which take into account the relative grid spacing at different center latitudes (ψ, in degrees; Jones et al. 2013).

In order to produce the classification for the entire globe, the center of the cross is displaced from one grid-box to another through all points of a reference 2.5° regular SLP grid within a band from 80°S to 80°N. Note that grid-boxes within 90°S–80°S and 80°N–90°N are beyond the range of the JC-WT method since the cross extends 10° north-south from its center (Fig. 1). The JC-WT method was conceived for extratropical application

since significant pressure gradients within the cross, required for a meaningful classification, are expected to occur mainly in these latitudes. Consequently, the JC-WT domain of analysis is recommended to any mid-to-high latitude region (∼ 30°–70°) by Jones et al. (2013). However, in this study we calculate the JC-WT classification beyond these latitudes to obtain a more complete picture of the geographical limits of applicability of the method, also considering for the first time a spatially continuous application over the southern hemisphere. Brands (2022) performs JC-WT classification over all cells in the northern hemisphere for the latitudes between 30° N and 70° N only. Note that the $z_w^\mp$ coefficients are undefined at $\psi = \pm 5°$ cross center latitudes (Table 1), and take nonphysical, negative values in between. Therefore, this latitudinal band has been excluded from our calculations.

The worldwide JC-WT method implementation here presented is available through the R package `transformeR` (v2.0.2, Iturbide et al. 2019). Its application is also illustrated
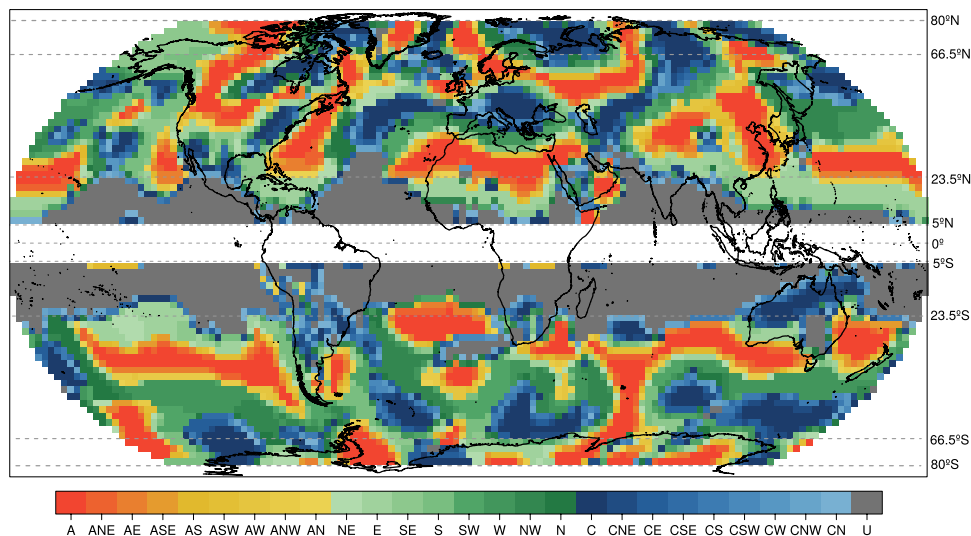
Fig. 2 Example of 6-hourly record of the Jenkinson-Collison Weather Type catalogue obtained from ERA-5, corresponding to the SLP state at {1979-01-01} 00:00:00 UTC. The 26 JC-WT circulation types are indicated in the legend, ranging from purely anticyclonic (A) and its hybrids (ANE to AN), pure directional (NE to N) and purely cyclonic (C) and its hybrids (CNE to CN). Type 27, unclassified (U), is depicted in grey. For reference, dashed grey lines depict some latitudes such as the Equator, the Tropic of Cancer (23.5° N) and Capricorn (23.5° S) and the Arctic and Antarctic Circles (± 66.5°), and they are also included in subsequent figures

through a worked example in the companion paper notebook (see Sec. Availability of data and materials).

2.2 Reanalysis data

We computed the global JC-WT classification using the 6-hourly SLP fields from five reanalysis products. Table 2 summarizes their features and provides references for further details. Prior to JC-WT application, all reanalyses were conservatively interpolated to a common 2.5° regular longitude-latitude grid (Fig. 1). In order to compare all reanalyses, we considered their common 27-year period 1979–2005, coincident with the AR5 CMIP5 historical baseline (Taylor et al. 2012). ERA-20C is produced through the assimilation of just SLP and marine winds, being therefore not fully comparable to the others, which assimilate a wider range of surface, upper-air and satellite observations. However, it has been also included in the intercomparison experiment for the sake of diversity. The reanalysis uncertainty is here analyzed by following an "all-against-all" validation scheme, so every reanalysis have been validated against each other.

2.3 Jenkinson–Collison classification assessment

2.3.1 Weather type frequencies and transition probabilities

One salient feature of a weather type is its probability of occurrence, which can be estimated by the relative frequency of occurrence in a sample, i.e. the proportion of 6-h records classified in a particular category over the complete time series length. JC-WT persistence or, more generally, transition probabilities between two different types are also important. They determine key temporal features such as spell duration, serving as an effective tool for the assessment of the model ability to reproduce circulation pattern sequences (Gibson et al. 2016; Hochman et al. 2019; Fernandez-Granja et al. 2021). In order to measure the differences among reanalyses, we assess both the JC-WT probabilities of occurrence for each individual type, as well as the probability of transition of one type into another. The latter are analysed using a transition probability matrix (TPM), briefly described next. Let the discrete random variable X_t represent a particular JC-WT at time t, whose values $x_t \in \{1, \ldots, K\}$, where $K = 27$ is the total number of WTs. We consider this variable at two consecutive time steps, X_{t-1} and X_t, to construct the $K \times K$ transition probability matrix A, where $A_{ij} = p(X_t = j \mid X_{t-1} = i)$, representing the probability of transitioning from WT i to WT j. Hence, each row of the matrix sums to one, $\sum_j A_{ij} = 1$. The TPM thus provides a visual "fingerprint" on how a given dataset reproduces the JC-WT classification when centered on a given grid cell. TPMs can be compared to a reference through specific evaluation measures (Sect. 2.3.2). Further details and examples of TPMs are presented in Fernandez-Granja et al. (2021).

2.3.2 Evaluation measures

Lamb weather types (and its automated interpretation from Jenkinson–Collison) method has proven to be useful for many regions in the Northern Hemisphere, ranging from maritime climates like the British Isles or the Iberian Peninsula (Jones et al. 1993; Trigo and DaCamara 2000) to extremely continental climates in central Asia (Wang et al. 2017). Furthermore, the JC-WTs can be linked to the variability in near-surface variables such as cloudiness, sunshine, wind-speed and even atmospheric chemistry (Brands et al. 2014) and the identification of wind storms in Central Europe (Donat et al. 2010). Sarricolea et al. (2018) investigated the JC-WTs associated with the teleconnections affecting central-southern Chile, namely El Niño Southern Oscillation (Trenberth 1997), Pacific Decadal Oscillation (Mantua and Hare 2002) and Antarctic Oscillation (Limpasuvan and Hartmann 1999) also known as Southern Annular Mode (Gong and Wang 1999). Similarly, in order to assess how meaningful the obtained JC-WTs all around the globe are, we identified the weather type yielding the strongest positive correlation with three main teleconnection indices, which largely affect climate variability in both hemispheres, namely the North Atlantic Oscillation, Pacific-North American Pattern (Barnston and Livezey 1987) and the Antarctic Oscillation. Our results corroborate the expected most frequent JC-WT linked to these teleconnections in large regions of the world (Fig. 11 in the Appendix) and are in line with previous studies based on mean sea-level pressure or geopotential height patterns (Barnston and Livezey 1987; Hurrell 1995; Gong and Wang 1999). Thus, we assume that the application the JC-WT classification is physically meaningful in large spatial domains of both hemispheres and in the following the limits of this applicability are examined in depth.

Two main aspects are addressed in our evaluation of the JC-WT classification. Firstly, we investigate the suitability of the method for each region of the world by using two criteria: (1) the number of different types, measuring the regional circulation's *diversity*, and (2) the occurrence of the Unclassified (U) type, witnessing weak pressure gradient with no clear vorticity tendency, also known as *barometric swamp* (Grimalt-Gelabert et al. 2013). Low diversity and frequent barometric swamp are here assumed to be indicative of the method working at its theoretical limits, i.e. in climate regimes for which it has not been developed; most prominently the monsoon and Intertropical Convergence Zone. Applying the method under these circumstance makes little sense since synoptic variability is either missing at the considered scale or it is represented by other variables than SLP. We here intentionally push the method to its limits in order to explore whether it can be applied anywhere in between 30 and 70 degrees North or South, as was estimated by Jones et al. (2013), or even beyond. For the diversity criterion, we consider weather types attaining relative frequencies above 0.1%, i.e. 40 or more occurrences in the total record of nearly 40,000 time steps. This threshold has been chosen since some JC-WTs were found to occur with relative frequencies as small as 0.47%

in its original formulation for the British Isles (Perry and Mayes 1998). In light of both measures (weather type diversity and type U frequency) jointly considered, we aim to obtain empirical evidence about the global geographical boundaries for the applicability of the JC-WT classification.

Secondly, reanalysis uncertainty is addressed. In order to evaluate the discrepancies among reanalyses, we measure the differences in their resulting JC-WT classification considering the relative bias of their WT frequencies, as well as the statistical significance of these differences using a two-proportions Z-test. Annual and seasonal relative biases for each WT are computed among all pairs of reanalyses in Table 2. The relative bias is a non-dimensional measure, which is zero for a perfect agreement of frequencies. The null hypothesis for the two-proportions Z-test is that the relative frequencies of a given type for two different reanalyses are the same. We use this parametric test in order to identify significant differences in their resulting weather type frequencies. Here, we use the Z-test implementation in the `prop.test` function from the R package `stats` (v3.6.3, R Core Team 2020), which includes an exact test for small samples, better suited for infrequent weather types. The test was performed using a 95% confidence level.

Reanalysis differences in their representation of transition probabilities were evaluated by the TPM Score (TPMS, Eq. 1), envisaged to provide a quantitative measure of dissimilarity between two transition probability matrices (Fernandez-Granja et al. 2021). TPMS is defined as follows:

$$TPMS = \sum_{p \in A^*} | p - p_{ref} | \tag{1}$$

where p and p_{ref} are the transition probabilities in the test and in the reference datasets, respectively. The (absolute) difference is calculated considering a subset of transition probabilities A^* from the full matrix (A), that are significantly different between the two reanalyses considered in each comparison, following the two-proportion Z-test. In order to include the "missing" transitions in the score (i.e. either transitions that exist in the reference but do not occur the test dataset, or transitions that occur in the test but do not in the reference dataset), these are assigned a zero probability (i.e. either $p = 0$ or $p_{ref} = 0$) and included in the A^* subset. As a result, the larger the TPMS departure from zero (perfect agreement), the larger the dissimilarity of the TPM fingerprints between the reanalyses for a given center grid cell.

2.4 Regional synthesis

Finally, in order to provide a synthetic overview of the main results, we provide a regional assessment of our results. To this aim, we use the latest set of climatic reference regions used in by the IPCC for the assessment of historical trends and future climate change projections (Iturbide et al. 2020). In order to avoid the inclusion of unsuitable areas for the application of

the JC-WT methodology and provide a more meaningful summary valid for regional intercomparison purposes, we exclude from the original polygon dataset the whole intertropical range ($23.5°S - 23.5°N$), thus producing a modification of some of the original IPCC regions to exclude this area. The IPCC regions affected are indicated with an asterisk throughout the text. The modified polygon layer is included as supplementary material of this study to ensure the reproducibility of the results (see Sect. Availability of data and materials).

3 Results and discussions

3.1 Suitability of the JC-WT classification worldwide

For brevity, the following results are based on ERA-5 unless otherwise indicated. The global distribution of the total number of distinct WTs (Fig. 3, left) shows a marked latitudinal gradient, with a decreasing diversity of types towards the tropics. Conversely, the frequency of the U type (Fig. 3, right) exhibits a sudden increase in the tropics, following a pattern similar to type diversity (left). In general, the lower the diversity of types, the higher the frequency of the U type, with a few regional exceptions, where reduced diversity coincides with small U numbers. Such exceptions are found year-round over Antarctica and the Tibetan Plateau; and to a lesser degree also over Greenland and the southern Indian Ocean at mid-latitudes.

Visual inspection of the maps in Fig. 3 reveals a remarkable empirical threshold of around 16 different types coinciding with at least half the temporal record falling into the U type. This threshold will be interpreted as applicability criterion in the forthcoming and is generally met polewards at the Tropics latitudes on both hemispheres ($\pm 23.5°$), which clearly extends the range of application suggested by Jones et al. (2013), from 30° to 70°.

The aforementioned thresholds exhibit seasonal excursions which affects the Mediterranean, Middle-East and southwestern United States during JJA season, as well as the mid-latitude eastern South Atlantic and eastern South Pacific for DJF. This seasonal fluctuations go hand in hand with the seasonal shifts of the Intertropical Convergence Zone (ITCZ, Barry and Carleton 2013), where local scale processes of deep convection are predominant and may alter to some extent the applicability of the JC-WT classification even in the extra-tropics.

In the Mediterranean Basin, for instance, suitability is optimal during DJF (boreal winter, maximum JC-WT diversity and a negligible type U frequency), which is due to a southward shift of the Atlantic storm tracks in combination with autochthonous cyclogenesis over the Mediterranean Sea (Fita et al. 2007). In JJA (boreal summer), however, the U type frequency increases in hand with a shrinking type diversity, hence compromising the usefulness of the classification during this season. Miró et al. (2020) used a modified version of the JC method, which
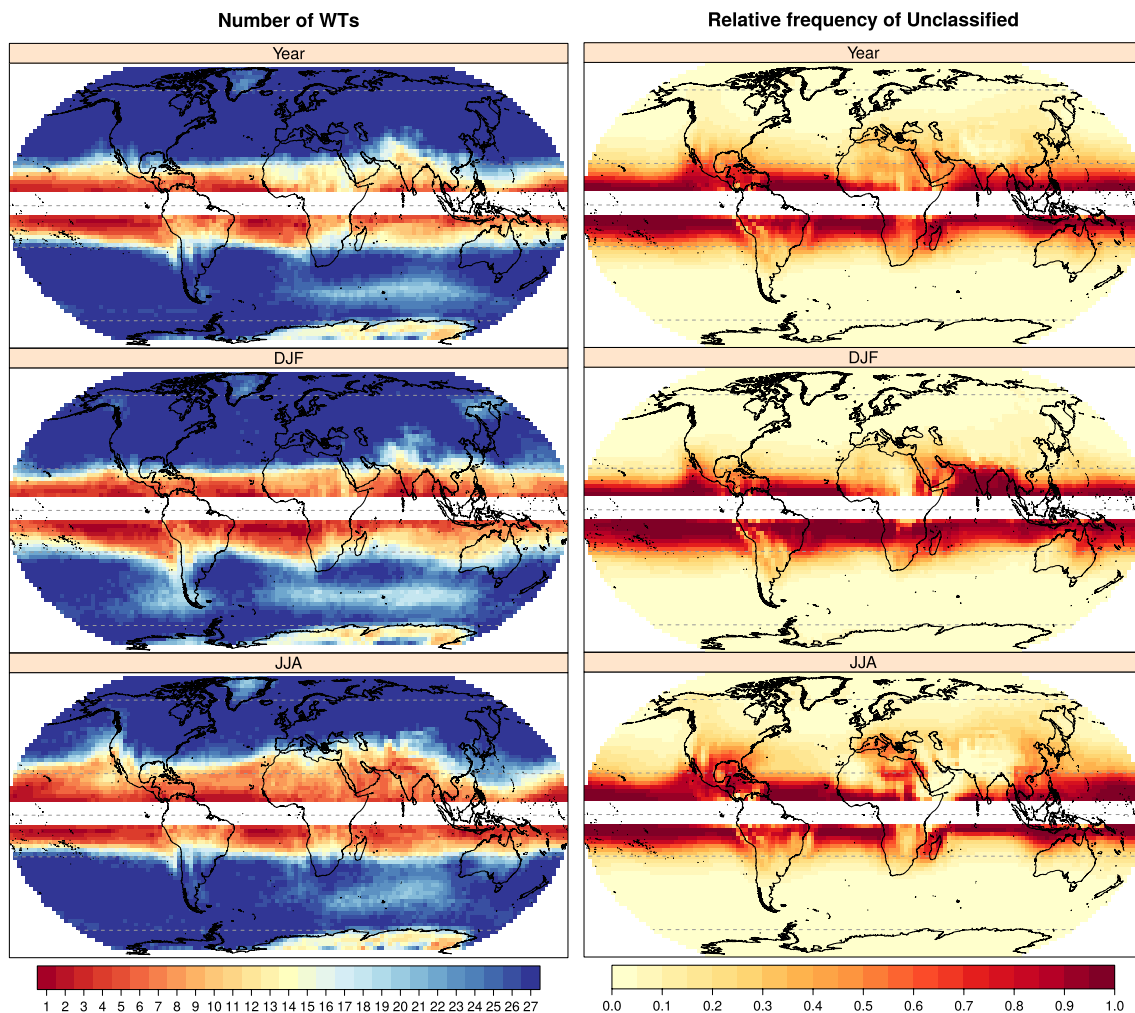
Fig. 3 Summary of the Jenkinson–Collison global classification calculated upon the SLP from ERA-5 (6-hourly, 1979–2005), considering the whole annual series (top row) and DJF and JJA seasons (rows 2–3 respectively). Left column: Number of weather types per grid-box with a relative frequency of occurrence above 0.1%. Right column: Relative frequency of the Unclassified type (U) per grid-box

combines the JC classification at the surface with an upper air classification based on 500 hPa geopotential height, obtaining a better differentiation within the U type, for a small region in the Pyrenees. Further research is needed for an overall and systematic application of this modified version, since expert local knowledge is needed to fine-tune the parameters. In summary, for both hemispheres, the favourable area widens towards the equator during their winter and retreats towards the respective pole during summer (Fig. 3).

3.2 Reanalysis uncertainty

After determining the regional applicability limits of the JC-WT classification, we next analyze its consistency among different reanalyses. In order to summarize the results, we will here refer to the modified IPCC-AR6 regions (Sect. 2.4, Fig. 4).

Overall, ERA-20C and ERA-Interim are more similar to ERA-5 than NCEP and JRA-55, as revealed by TPMS (Figs. 4 and 10 in the Appendix). For the latter two datasets, large TPMS values are obtained over Greenland (GIC), Antarctica (WAN, EAN), Northern Central-America (NCA*), West North-America (WNA), Central North-America (CNA), central Asia (WCA, ECA, EAS), Southern Asia (SAS*) and the Tibetan Plateau (TIB), where values in excess of 10 are found. In the Southern Hemisphere, large discrepancies between reanalyses are found over South America (SWS* and SES regions). The above mentioned regions present complex orography, with high-altitude mountain systems such as the Himalayas, the Andes and the Rocky Mountains or thick ice sheets like Antarctica and Greenland. The discrepancies found in these regions of complex terrain are likely related to the differences in the SLP fields from the reanalyses (Fig. 8 in the Appendix), estimated from pressure

reduction algorithms that are very sensitive to the representation of orography and its spatial resolution (Sterl 2004; Lavin-Gullon et al. 2021; Brands 2022,e.g.). The magnitude of these differences is potentially large and can reach several hPa in certain areas (Fita et al. 2019). They can be particularly critical for Antarctica, which is mostly ice sheet several kilometers high. Therefore, the poor representation of the SLP by the different reanalyses prevents from the application of JC-WTs classification in these regions, as reflected by their high TPMS values (Fig. 4).

The seasonal analysis of the TPMS between JRA-55 and ERA-5 (Fig. 5) generally reveals a seasonal march of the largest values towards the pole of the summer hemisphere. This is similar to the results found for type diversity and U frequency (Sect. 3.1), where the ITCZ may determine the JC-WT applicability to some point in that oscillating stripe.

In particular, the seasonal TPMS values for North Central-America (NCA*) and the Sahara region (SAH*) are larger than the annual ones (Fig. 5). In the Mediterranean (MED), Central North-America (CNA) and in West North-America (WNA), the TPMS values are largest in JJA and lowest in DJF. Reflecting the aforementioned seasonal march, the TPMS values for South South-America (SSA), West South-Africa (WSAF*), East South-Africa (ESAF*), Madagascar (MDG*) and Central Australia (CAU) reach their maximum in DJF, with a much larger magnitude than in any other season.

According to Fig. 5, moderately high TPMS values are found year-round in the mid-latitude Indian Ocean, which extend to the

eastern South Atlantic and eastern South Pacific during DJF (austral summer), particularly affecting the Southern-Ocean (SOO) region. These differences might be caused by scarce observations in that area and, noteworthy, they again coincide with a relatively low type diversity, as reported in the previous section.

The large TPMS values found along the margins of the East Antarctic Ice Sheet (EAIS) are probably related to an abrupt shift of the easterly katabatic winds blowing down the ice sheet to quasi-persistent westerlies at mid-latitudes, driving the Antarctic Ocean divergence zone (Davis and McNider 1997). This singular regional modulation of the wind field might by resolved in a distinct manner by the two reanalyses and so is the pressure reduction to mean sea-level over the ice sheet itself. Notably, the TPMS values over the West Antarctic Ice Sheet are systematically lower than those over the EAIS (compare WAN to EAN regions respectively).

In order to shed some light on regional TPMS, we investigate the relative biases of WTs frequencies for each IPCC region, which reveal misrepresentations of the synoptic conditions and their frequencies by the applied reanalyses. As an illustrative example, we show the results for the Mediterranean (MED) region in Fig. 6. The respective results for the remaining IPCC regions can be obtained by following the working example on analysis reproducibility indicated in Sect. Availability of data and materials.

Results show biases of different magnitude and sign, depending on the reanalysis. The majority of statistically significant
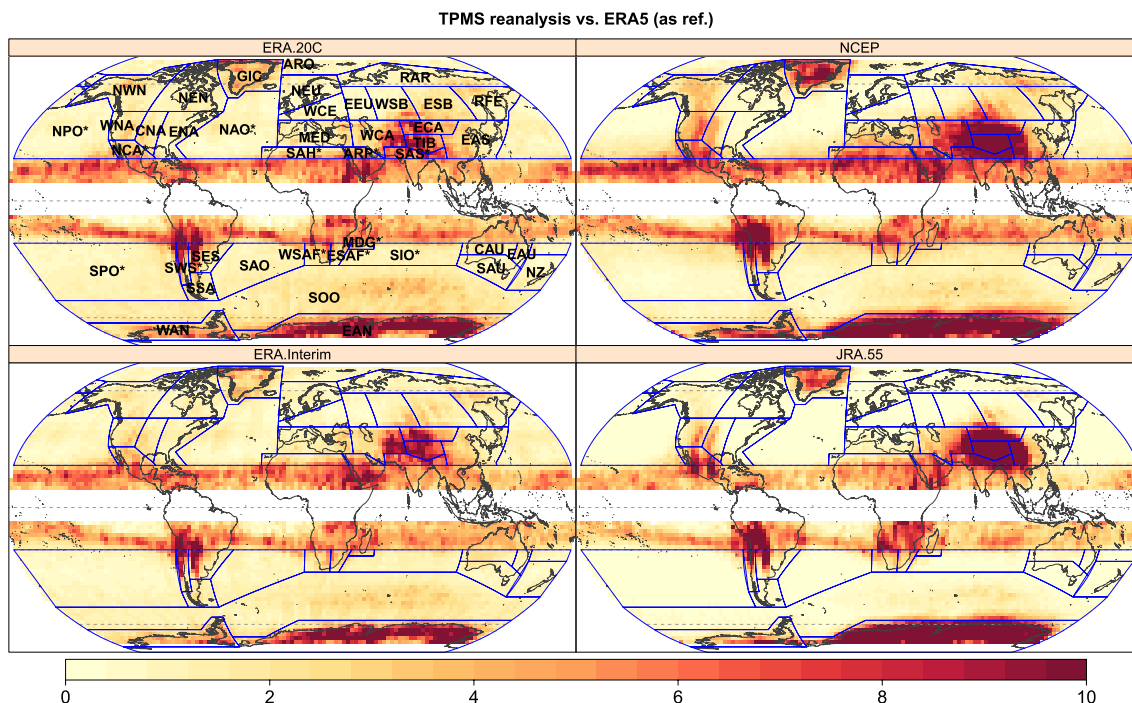
Fig. 4 Annual Transition Probability Matrix Scores (TPMS, Sect. 2.3.2) of NCEP, ERA-Interim, ERA-20C and JRA-55 against ERA-5 (used as reference). The modified IPCC region polygon layer with the region identification codes are depicted in the top-left. Note that the original IPCC regions that have been modified to exclude the intertropical range (see Sect. 2.4) are marked with an asterisk
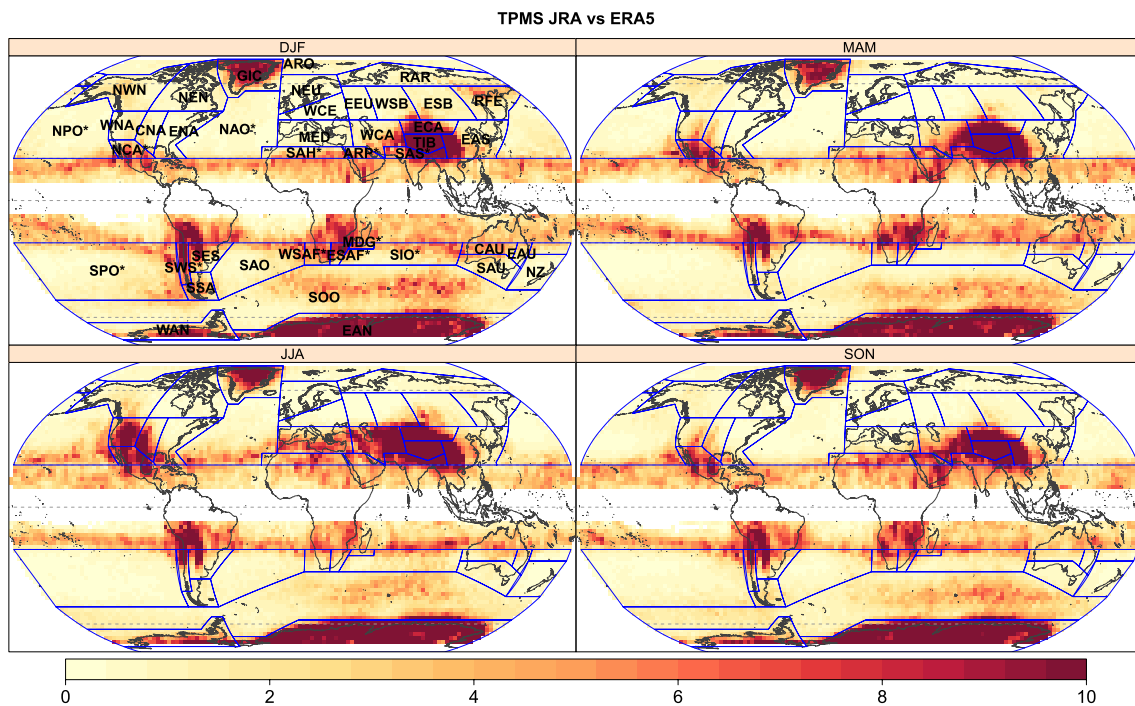
Fig. 5 Seasonal transition probability matrix scores (TPMS, Sect. 2.3.2) of JRA-55 reanalysis against ERA-5 (reference)

differences (marked with asterisks) occur for the most frequent WTs (see WTs frequencies for ERA-5 in the right panel). The largest and most significant biases are found during JJA, which coincides with large TPMS values (Fig. 5). For the least frequent weather types, reanalyses do not exhibit significant differences with respect to ERA-5, especially in spring, autumn and for the annual results. The Unclassified type is the most frequent one in all seasons except DJF. It exhibits significant differences among reanalyses in all seasons, especially during JJA and SON.

All in all, we found a relationship between three factors, namely large values of TPMS (Figs. 4 and 5), small number of WTs and high frequency of the U type (Fig. 3). These three factors should be analyzed together due to the fact that large TPMS in some regions might come from the limitations in the suitability of the JC-WT classification. In other regions where the classification method is suitable, the TPMS purely reflects the uncertainty among reanalyses. However, the relationship seems to be clearer between large TPMS and low number of LWTs. Figure 7 summarizes Figs. 3, 4 and 5 for all the IPCC regions and analizes the connection between the number of distinct WTs and TPMS.

Considering the criteria of JC-WT diversity, the method might be less suitable for regions like SAS* and EAN, where few distinct WTs appear (median below 16 types). Seasonally, other regions also stand out by their low number of WTs, e.g. CAU or WSAF* in boreal winter and TIB, ARP*, SAH*, NCA* and WCA in boreal summer (Fig. 7). There is a large spatial variability in terms of WTs diversity in some regions where the applicability of the WT classification is

questionable, such as EAN, TIB, ARP*, SAH* or WSAF*. Regardless of their median number of WTs, these regions show grid cells where all WTs are registered. Additionally, there are some regions that stand out for having large TPMS (i.e. reanalysis uncertainty) despite of their large number of WTs: EAN, NCA*, SWS*, ESAF*, SES, EAS, ECA and GIC; only in DJF we can add TIB, SSA and WAN; and only in JJA we can add MED, WNA and CNA.

4 Conclusions

In the present study, we assess the potential applicability of JC-WT classification for the entire world, except the inner tropics. Furthermore, we evaluate the consistency of the JC-WTs classifications obtained from five different state-of-the-art reanalysis products of varying characteristics and resolutions by means of the TPMS and relative bias in the WTs frequencies. To this aim, we first formulate a modification of JC-WT method to allow for its use in the Southern Hemisphere and then use two different criteria to evaluate its applicability worldwide: the number of JC-WTs reflecting "type diversity" and the relative frequency of the Unclassified type. A roll-out of up to 41 regions extracted from the latest set of IPCC Working Group I reference regions has been used to divide the globe in order to address these analyses on the regional scale.

We show that the JC-WT approach can be reliably applied over most of the global areas within 23.5° and 80° latitude on
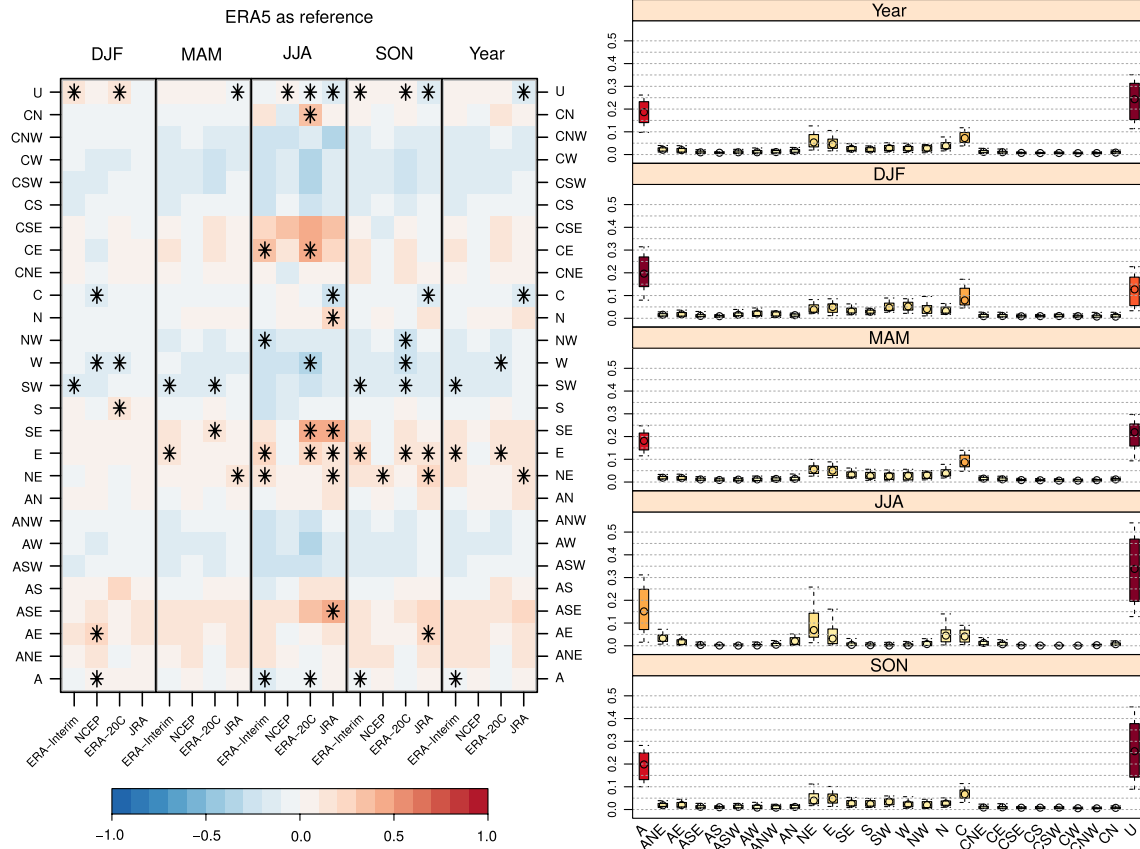
Fig. 6 Left: Annual and seasonal relative biases of weather type frequencies for the different reanalyses (in columns) against ERA-5 (reference) for MED. Asterisks indicate statistically significant differences following the two proportion Z-test (Sect. 2.3.2). Right: Annual and seasonal regional weather type frequencies as represented by

ERA-5 for MED, used as reference for the relative biases on the left. The boxes represent the spatial variability of type frequencies within MED, where the box upper/lower boundaries show the inter-quartile range and the lower/upper whiskers extend to the 10th and 90th percentiles respectively. Circles indicate the median frequency

both hemispheres. For most of this area of applicability, we find a large diversity of WTs, while the type U (representing null pressure gradient situations) occurs with low frequency. As a warning of the loss of applicability of the method, we find a transition from which the diversity of WTs decreases sharply at the same time that the type U becomes the dominant type. This transition marks an empirical applicability threshold of 16 distinct WTs.

The TPMS maps, which provide a measure of WTs transition probability agreement, unveil a general consistency between reanalyses within this applicability range. On the one hand, there are regions where the JC-WT approach is in principle applicable but its practical use is hampered by a large reanalysis uncertainty. These are the Mediterranean (MED) in JJA, and Madagascar (MDG*) and East Southern-Africa (ESAF*) in DJF. On the other hand, there are regions where JC-WT is less suitable irrespective of the reanalysis uncertainty. These are Arabian-Peninsula (ARP*) and SAHara (SAH*) in JJA, and West Southern-Africa

(WSAF*) and Central Australia (CAU) in DJF. Likewise, there are regions with complex orography where the JC-WT classification should be taken with caution as the SLP is estimated through pressure reduction algorithms, differently for each dataset. Our analyses confirm the expected large discrepancies among reanalyses there: Greenland (GIC), Antarctica (WAN, EAN), Northern Central-America (NCA*), West North-America (WNA), Central North-America (CNA), central Asia (WCA, ECA, EAS), Southern Asia (SAS*) and the Tibetan Plateau (TIB).

Both the 16-type diversity threshold and large TPMS areas exhibit a seasonal march towards the pole of the respective summer hemisphere. This excursion is particularly strong for the TPMS during JJA (boreal summer).

Generally, ERA-20C, ERA-Interim and ERA-5 represent more similar transition probabilities than NCEP and JRA-55, in accordance with their respective similarities in terms of SLP fields, specially in areas of complex orography.
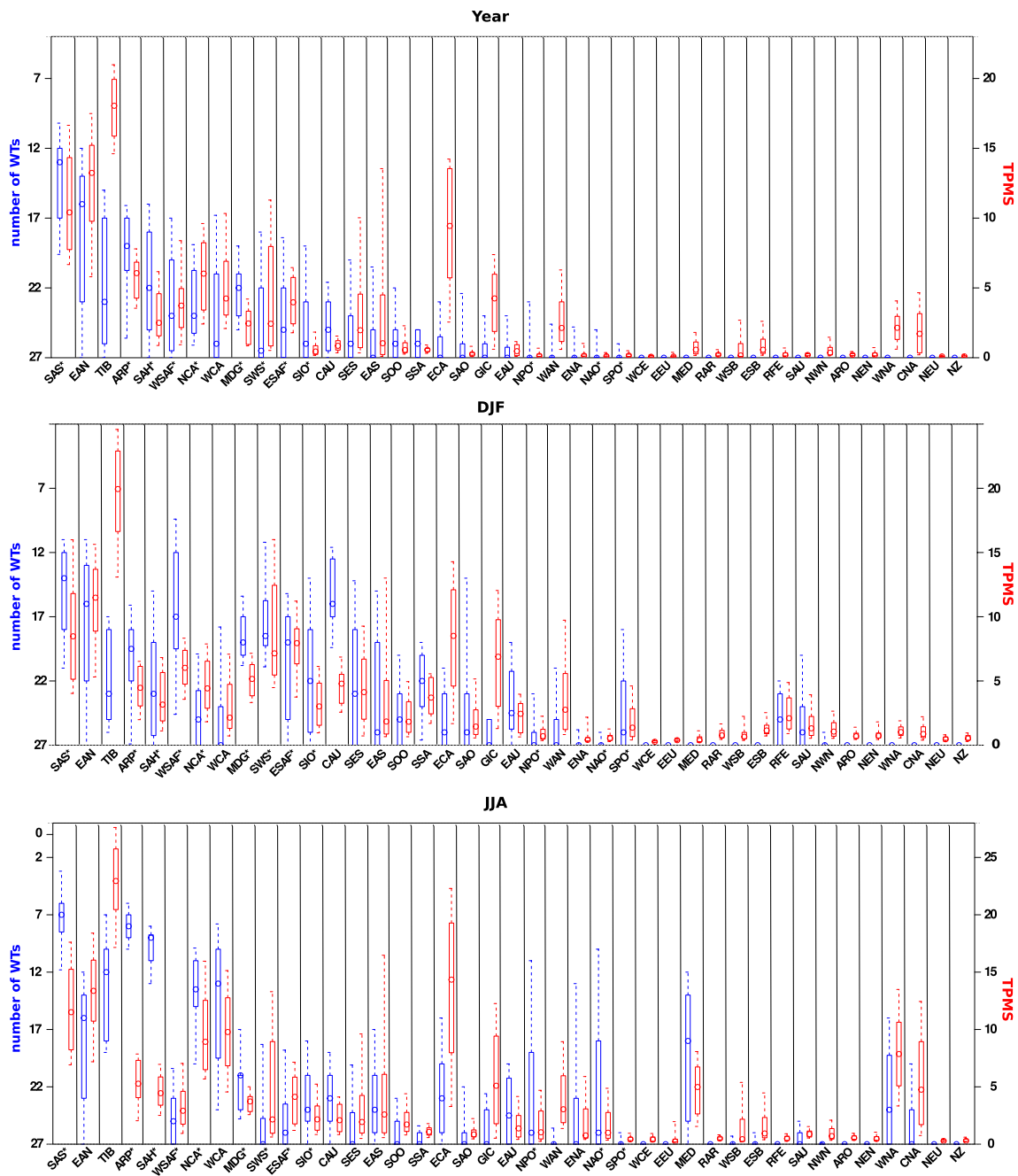
Fig. 7 TPMS (in red) of JRA-55 against ERA-5 and the number of WTs (in blue) of ERA-5 for each IPCC region. The three different panels correspond to annual, DJF and JJA. The limits of the boxes show the spatial interquartile range and whiskers depict the 10th and 90th percentile. The median values are represented with a circle inside the boxes. In the three panels, regions are sorted by decreasing order of the 75th percentile of the number of WTs at annual scale

This is the first study addressing the global application of the JC-WTs. We define its limits of applicability, providing an extension of this popular classification method that can serve as a potential tool for process-based climate model evaluation.

Appendix A: Differences in sea-level pressure

Differences in the sea-level pressure (SLP) fields between reanalyses (ERA-5 is used as reference) can be found in Figs. 8 and 9.
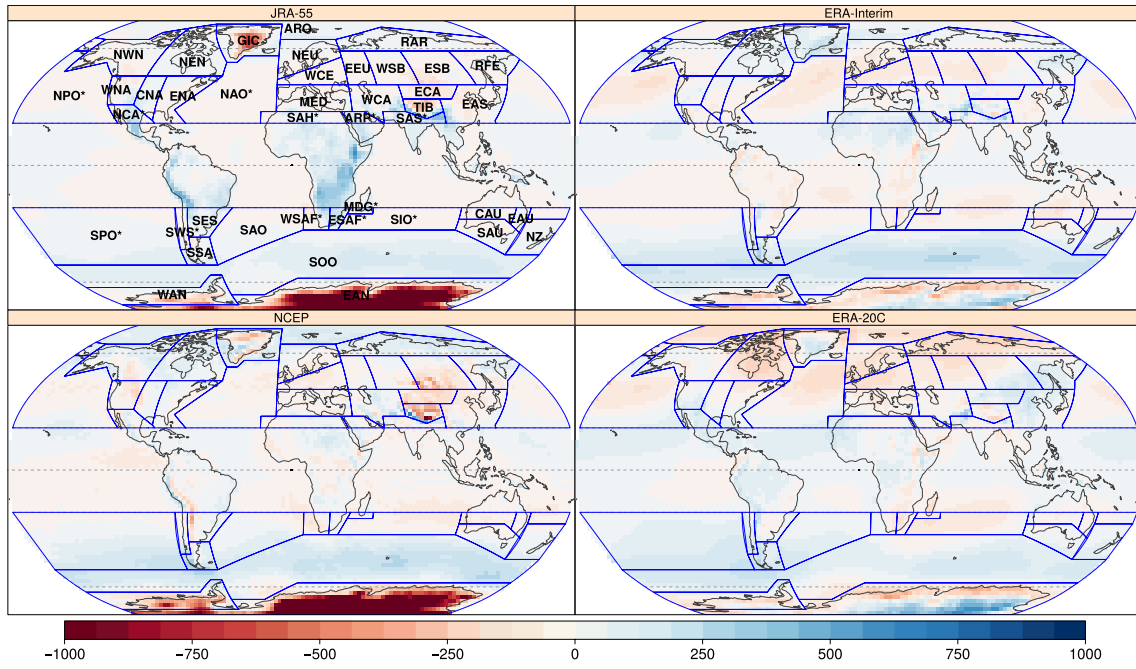
Fig. 8 SLP annual mean difference (Pa) with respect to ERA-5 (1979–2005)
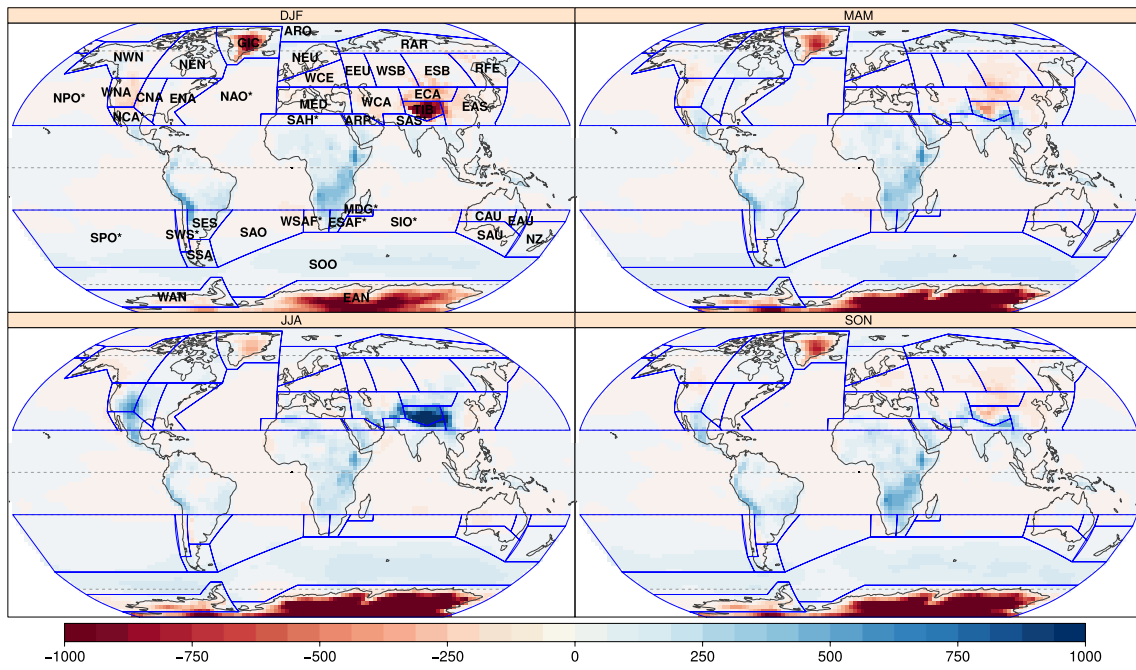
Fig. 9 Similarly to Fig. 8, seasonal mean difference (Pa) of SLP in JRA-55 with respect to ERA-5 (1979–2005)

Appendix B: TPMS for other reanalysis pairs

TPMS calculated for the remaining pairs of reanalyses can be found in Fig. 10.
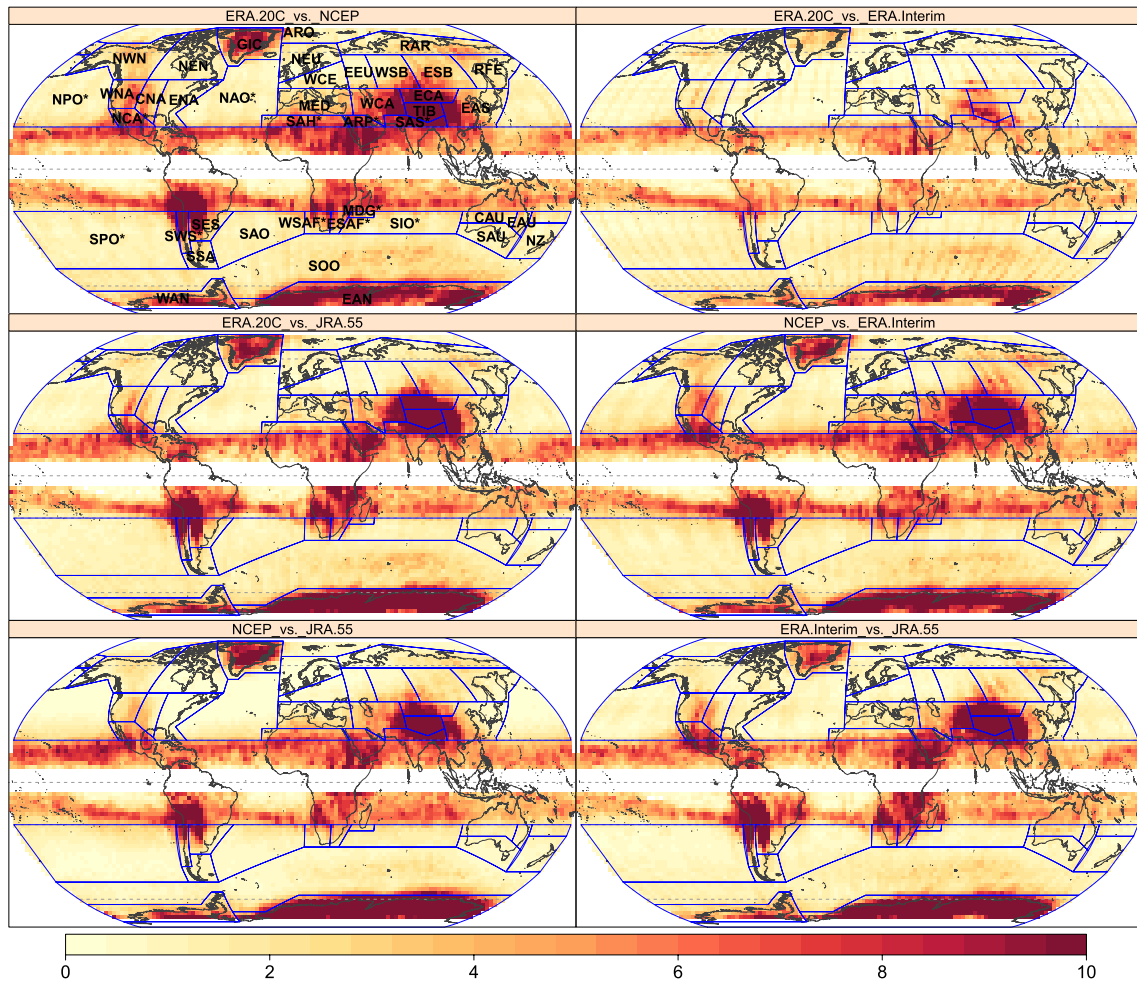
Fig. 10 Annual TPMS calculated between different reanalysis pairs (specific pairs are found in the sub-panels titles). IPCC regions short names can be seen in the top-left sub-panel

Appendix C: Correlation of JC-WTs frequencies with teleconnections

Weather types yielding the strongest positive correlation with three main teleconnection indices are found in Fig. 11.
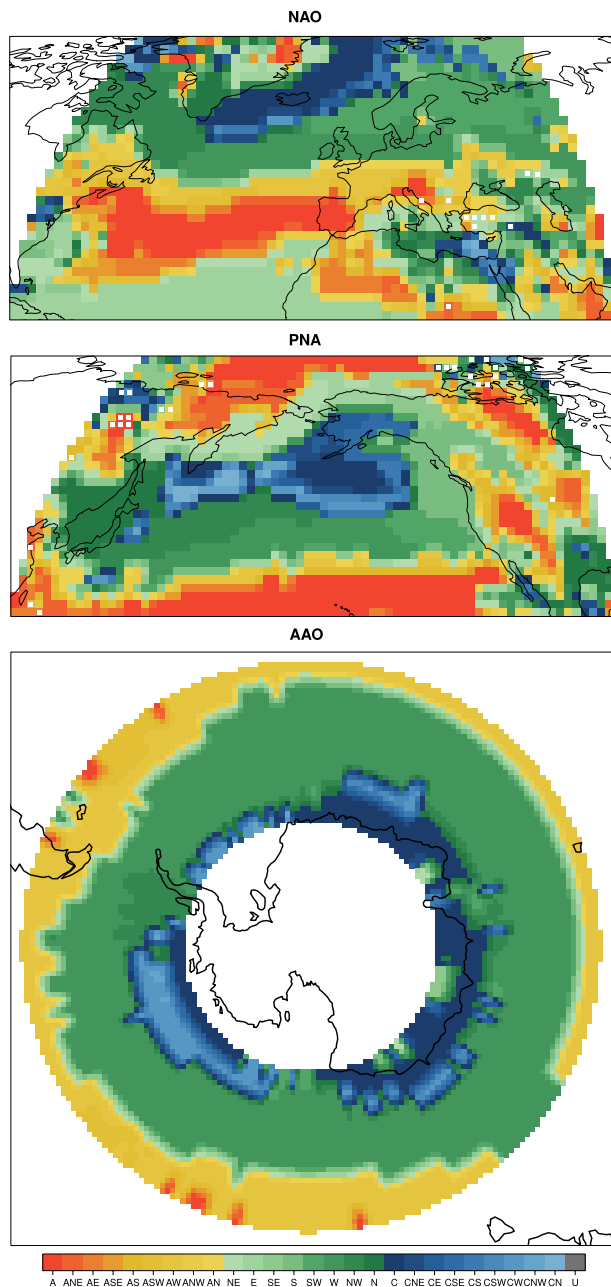
Fig. 11 Jenkinson–Collison weather type yielding the strongest positive correlation coefficient with the North Atlantic Oscillation (NAO), Pacific-North American Pattern (PNA) and Antarctic Oscillation (AAO) indices at each grid-box of the North Atlantic-European domain, North Pacific region and between 50° and 70° South, respectively. Non-statistically significant correlations (at a confidence level of 95 %) are marked with a white box. Monthly JC-WT frequencies and index values are taken into account. JC-WTs are derived from the ERA-5 reanalysis (1979–2005)

Declarations

Conflict of interest The authors declare no competing interests.

References

Barnston AG, Livezey RE (1987) Classification, seasonality and persistence of low-frequency atmospheric circulation patterns. Monthly Weather Rev 115(6):1083–1126 https://doi.org/10.1175/1520-0493(1987)115h1083:555 CSAPOLi2.0.CO;2, url: journals.ametsoc.org/view/journals/mwre/115/6/1520-0493_1987_115_1083_csapol_2_0_co_2.xml

Barriopedro D, Fischer EM, Luterbacher J et al (2011) The hot summer of 2010: redrawing the temperature record map of Europe. Science 332(6026):220–224. https://doi.org/10.1126/science.1201224

Barry RG, Carleton AM (2013) Synoptic and dynamic climatology. Routledge

Ben Daoud A, Sauquet E, Lang M et al (2009) Comparison of 850-hPa relative humidity between ERA-40 and NCEP/NCAR re-analyses: detection of suspicious data in ERA-40. Atmos Sci Lett 10(1):43–47 https://doi.org/10.1002/asl.208 url: hal-insu.archives-ouvertes.fr/insu-00411903

Bengtsson L (2004) Can climate trends be calculated from reanalysis data? J Geophys Res 109(D11):D11,111. https://doi.org/10.1029/2004JD004536, http://doi.wiley.com/10.1029/2004JD004536

Bladé I, Liebmann B, Fortuny D et al (2011) Observed and simulated impacts of the summer NAO in Europe: implications for projected drying in the Mediterranean region. Clim Dyn 39(3–4):709–727. https://doi.org/10.1007/s00382-011-1195-x

Brands S (2022) A circulation-based performance atlas of the cmip5 and 6 models for regional climate studies in the northern hemisphere. Geosci Model Dev Discuss pp 1–48. https://doi.org/10.5194/gmd-2020-418, https://gmd.copernicus.org/preprints/gmd-2020-418/

Brands S, Gutiérrez JM, Herrera S et al (2012) On the use of reanalysis data for downscaling. J Clim 25(7):2517–2526 https://doi.org/10.1175/JCLI-D-11-00251.1 journals.ametsoc.org/view/journals/clim/25/7/jcli-d-11-00251.1.xml

Brands S, Herrera S, Gutiérrez J (2014) Is Eurasian snow cover in October a reliable statistical predictor for the wintertime climate on the Iberian peninsula? Int J Climatol 34(5):1615–1627. https://doi.org/10.1002/joc.3788

Buehler T, Raible CC, Stocker TF (2011) The relationship of winter season North Atlantic blocking frequencies to extreme cold or dry spells in the ERA-40. Tellus A: Dyn Meteorol Oceanogr 63(2):174–187. https://doi.org/10.1111/j.1600-0870.2010.00492.x

Busuioc A, Chen D, Hellström C (2001) Performance of statistical downscaling models in GCM validation and regional climate change estimates: application for Swedish precipitation: STATISTICAL DOWNSCALING FOR SWEDISH PRECIPITATION. Int J Climatol 21(5):557–578. https://doi.org/10.1002/joc.624

Casanueva A, Rodríguez-Puebla C, Frías MD et al (2014) Variability of extreme precipitation over Europe and its relationships with teleconnection patterns. Hydrol Earth Syst Sci 18(2):709–725. https://doi.org/10.5194/hess-18-709-2014

Chen D (2000) A monthly circulation climatology for Sweden and its application to a winter temperature case study. Int J Climatol 20:1067–1076. https://doi.org/10.1002/1097-0088(200008)20:103.0.CO;2-Q

Chen J, Del Genio AD, Carlson BE et al (2008) The spatiotemporal structure of twentieth-century climate variations in observations and reanalyses. Part I: long-term trend. J Clim 21(11):2611–2633. https://doi.org/10.1175/2007JCLI2011.1, http://journals.ametsoc.org/doi/10.1175/2007JCLI2011.1

Conway D, Jones P (1998) The use of weather types and air flow indices for GCM downscaling. J Hydrol 212:348–361

Davis A, McNider R (1997) The development of Antarctic katabatic winds and implications for the coastal ocean. J Atmos Sci 54(9):1248–1261

Dee DP, Uppala SM, Simmons AJ et al (2011) The ERA-Interim reanalysis: configuration and performance of the data assimilation system. Q J R Meteorol Soc 137:553–597. https://doi.org/10.1002/qj.828

Dey R, Lewis SC, Arblaster JM et al (2019) A review of past and projected changes in Australia's rainfall. Wiley Interdiscip Rev Clim Change 10(3):e577

Donat MG, Leckebusch GC, Pinto JG et al (2010) Examination of wind storms over central Europe with respect to circulation weather types and NAO phases. Int J Climatol 30(9):1289–1300. https://doi.org/10.1002/joc.1982,

Favá V, Curto JJ, Llasat MC (2015) Relationship between the summer NAO and maximum temperatures for the Iberian Peninsula. Theor Appl Climatol. https://doi.org/10.1007/s00704-015-1547-2

Fealy R, Mills G (2018) Deriving lamb weather types suited to regional climate studies: a case study on the synoptic origins of precipitation over ireland. Int J Climatol. https://doi.org/10.1002/joc.5495

Fernandez-Granja JA, Casanueva A, Bedia J et al (2021) Improved atmospheric circulation over Europe by the new generation of cmip6 earth system models. Clim Dyn. https://doi.org/10.1007/s00382-021-05652-9

Fita L, Romero R, Luque A et al (2007) Analysis of the environments of seven Mediterranean tropical-like storms using an axisymmetric, nonhydrostatic, cloud resolving model. Nat Hazards Earth Syst Sci 7(1):41–56 https://doi.org/10.5194/nhess-7-41-2007, URL: nhess.copernicus.org/articles/7/41/2007/

Fita L, Polcher J, Giannaros TM et al (2019) CORDEX-WRF v1.3: development of a module for the weather research and forecasting (WRF) model to support the CORDEX community. Geosci Model Dev 12(3):1029–1066. https://doi.org/10.5194/gmd-12-1029-2019

Folland CK, Knight J, Linderholm HW et al (2009) The Summer North Atlantic Oscillation: past, present, and future. J Clim 22(5):1082–1103. https://doi.org/10.1175/2008JCLI2459.1

Fujiwara M, Wright JS, Manney GL et al (2017) Introduction to the sparc reanalysis intercomparison project (s-rip) and overview of the reanalysis systems. Atmos Chem Phys 17(2):1417–1452 https://doi.org/10.5194/acp-17-1417-2017, URL: acp.copernicus.org/articles/17/1417/2017/

Gettelman A, Rood RB (2016) Model evaluation. In: Gettelman A, Rood RB (eds) Demystifying climate models: a users guide to earth system models Earth systems data and models. Springer, Berlin, Heidelberg, pp 161–176. https://doi.org/10.1007/978-3-662-48959-8_9

Gibson PB, Uotila P, Perkins-Kirkpatrick SE et al (2016) Evaluating synoptic systems in the cmip5 climate models over the Australian region. Clim Dyn 47(7):2235–2251

Gibson PB, Waliser DE, Lee H et al (2019) Climate model evaluation in the presence of observational uncertainty: precipitation indices over the contiguous United States. J Hydrometeorol 20(7):1339–1357 https://doi.org/10.1175/JHM-D-18-0230.1, url: journals.ametsoc.org/doi/10.1175/JHM-D-18-0230.1

Gong D, Wang S (1998) Antarctic oscillation: concept and applications. Chin Sci Bull 43(9):734–738

Gong D, Wang S (1999) Definition of Antarctic oscillation index. Geophys Res Lett 26(4):459–462

Grimalt-Gelabert M, Tomas-Burguera M, Alomar-Garau G et al (2013) Determination of the Jenkinson and Collison's weather types for the western Mediterranean basin over the 1948–2009 period: temporal analysis. Atmosfera 26:75–94. https://doi.org/10.1016/S0187-6236(13)71063-4

Harada Y, Kamahori H, Kobayashi C et al (2016) The JRA-55 reanalysis: Representation of atmospheric circulation and climate variability. J Meteorol Soc Japan Ser II 94(3):269–302. https://doi.org/10.2151/jmsj.2016-015

Hersbach H, Bell B, Berrisford P et al (2020) The era5 global reanalysis. Q J R Meteorol Soc 146(730):1999–2049

Hochman A, Alpert P, Harpaz T et al (2019) A new dynamical systems perspective on atmospheric predictability: Eastern Mediterranean weather regimes as a case study. Sci Adv 5(6):eaau0936. https://doi.org/10.1126/sciadv.aau0936

Hulme M, Briffal K, Jones P et al (1993) Validation of GCM control simulations using indices of daily airflow types over the British isles. Clim Dyn 9(2):95–105. https://doi.org/10.1007/BF00210012

Hurrell JW (1995) Decadal trends in the north atlantic oscillation: Regional temperatures and precipitation. Science 269(5224):676–679 https://doi.org/10.1126/science.269.5224.676, www.science.org/doi/abs/10.1126/science.269.5224.676

Hurrell JW, Kushnir Y, Ottersen G et al (2003) An overview of the North Atlantic Oscillation. In: Hurrell JW, Kushnir Y, Ottersen G et al (eds) Geophysical monograph series, vol 134. American Geophysical Union, Washington, pp 1–35

Huth R, Nemesova I, Klimperová N (1993) Weather categorization based on the average linkage clustering technique: an application to European mid-latitudes. Int J Climatol 13(8):817–835. https://doi.org/10.1002/joc.3370130802

Huth R, Beck C, Philipp A et al (2008) Classifications of atmospheric circulation patterns: recent advances and applications. Ann N Y Acad Sci 1146:105–152. https://doi.org/10.1196/annals.1446.019

Iturbide M, Bedia J, Herrera S et al (2019) The R-based climate4R open framework for reproducible climate data access and post-processing.

Environ Model Softw 111:42–54. https://doi.org/10.1016/j.envsoft.2018.09.009

Iturbide M, Gutiérrez JM, Alves LM et al (2020) An update of ipcc climate reference regions for subcontinental analysis of climate model data: definition and aggregated datasets. Earth Syst Sci Data 12(4):2959–2970, https://doi.org/10.5194/essd-12-2959-2020, url:essd.copernicus.org/articles/12/2959/2020/

Jenkinson A, Collison F (1977) An initial climatology of gales over the north sea. Synoptic climatology branch memorandum. Meteorol Off 62

Jones PD, Hulme M, Briffa KR (1993) A comparison of Lamb circulation types with an objective classification scheme. Int J Climatol 13(6):655–663. https://doi.org/10.1002/joc.3370130606

Jones PD, Harpham C, Briffa KR (2013) Lamb weather types derived from reanalysis products. Int J Climatol 33(5):1129–1139. https://doi.org/10.1002/joc.3498

Jury MW, Herrera S, Gutiérrez JM et al (2019) Blocking representation in the ERA-Interim driven EURO-CORDEX RCMs. Clim Dyn 52(5–6):3291–3306. https://doi.org/10.1007/s00382-018-4335-8

Kalnay E, Kanamitsu M, Kistler R et al (1996) The NCEP/NCAR 40-year reanalysis project. Bull Am Meteorol Soc 77(3):437–472. https://doi.org/10.1175/1520-0477(1996)077<0437:TNYRP>2.0.CO;2

Kobayashi S, Ota Y, Harada Y et al (2015) The JRA-55 reanalysis: general specifications and basic characteristics. J Meteorol Soc Japan Ser II 93(1):5–48. https://doi.org/10.2151/jmsj.2015-001

Kotlarski S, Szabó P, Herrera S et al (2019) Observational uncertainty and regional climate model evaluation: a pan-European perspective. Int J Climatol 39(9):3730–3749 https://doi.org/10.1002/joc.5249, url:onlinelibrary.wiley.com/doi/10.1002/joc.5249

Lamb H (1972) British isles weather types and a register of daily sequence of circulation patterns 1861–1971. Meteorol Off Geophys Mem 116:1–85

Lavin-Gullon A, Feijoo M, Solman S et al (2021) Synoptic forcing associated with extreme precipitation events over southeastern south America as depicted by a cordex fps set of convection-permitting rcms. Clim Dyn 56(9):3187–3203

Limpasuvan V, Hartmann DL (1999) Eddies and the annular modes of climate variability. Geophys Res Lett 26(20):3133–3136 https://doi.org/10.1029/1999GL010478, url: agupubs.onlinelibrary.wiley.com/doi/abs/10.1029/1999GL010478

Littmann T (2000) An empirical classification of weather types in the Mediterranean basin and their interrelation with rainfall. Theor Appl Climatol 66(3–4):161–171. https://doi.org/10.1007/s007040070022

Mantua NJ, Hare SR (2002) The pacific decadal oscillation. J Oceanogr 58(1):35–44. https://doi.org/10.1023/A:1015820616384

Maraun D, Shepherd TG, Widmann M et al (2017) Towards process-informed bias correction of climate change simulations. Nat Clim Change 7(11):664–773. https://doi.org/10.1038/nclimate3418

Miró J, Pepin N, Peña J et al (2020) Daily atmospheric circulation patterns for Catalonia (Northeast Iberian Peninsula) using a modified version of jenkinson and collison method. Atmos Res 231(104):674

Otero N, Sillmann J, Butler T (2018) Assessment of an extended version of the Jenkinson-Collison classification on cmip5 models over Europe. Clim Dyn. https://doi.org/10.1007/s00382-017-3705-y

Perry M, Mayes J (1998) The lamb weather type catalogue. Weather 53(7):222–229. https://doi.org/10.1002/j.1477-8696.1998.tb06387.x

Pickler C, Mölg T (2021) General circulation model selection technique for downscaling: exemplary application to East Africa. J Geophys Res Atmos 126(6). https://doi.org/10.1029/2020JD033033, https://onlinelibrary.wiley.com/doi/10.1029/2020JD033033

Poli P, Hersbach H, Dee DP et al (2016) ERA-20C: an atmospheric reanalysis of the twentieth century. J Clim 29(11):4083–4097. https://doi.org/10.1175/JCLI-D-15-0556.1

Putnikovic S, Tosic I, Durdevic V (2016) Circulation weather types and their influence on precipitation in Serbia. Meteorol Atmos Phys. https://doi.org/10.1007/s00703-016-0432-6

R Core Team (2020) R: a language and environment for statistical computing. R Foundation for Statistical Computing, Vienna, Austria, https://www.R-project.org/

Ramos AM, Cortesi N, Trigo RM (2014) Circulation weather types and spatial variability of daily precipitation in the Iberian Peninsula. Front Earth Sci. https://doi.org/10.3389/feart.2014.00025

Rex DF (1950) Blocking action in the middle troposphere and its effect upon regional climate. Tellus 2(3):196–211. https://doi.org/10.1111/j.2153-3490.1950.tb00331.x

Risbey JS, Pook MJ, McIntosh PC et al (2009) On the remote drivers of rainfall variability in Australia. Mon Weather Rev 137(10):3233–3253

Sarricolea P, Meseguer-Ruiz O, Martin-Vide J et al (2018) Trends in the frequency of synoptic types in central-southern Chile in the period 1961–2012 using the Jenkinson and Collison synoptic classification. Theor Appl Climatol. https://doi.org/10.1007/s00704-017-2268-5

Schaller N, Sillmann J, Anstey J, et al (2018) Influence of blocking on Northern European and Western Russian heatwaves in large climate model ensembles. Environ Res Lett 13(5):054,015. https://doi.org/10.1088/1748-9326/aaba55, https://iopscience.iop.org/article/10.1088/1748-9326/aaba55

Sillmann J, Croci-Maspoli M (2009) Present and future atmospheric blocking and its impact on European mean and extreme climate. Geophys Res Lett 36(10):L10702. https://doi.org/10.1029/2009GL038259

Sousa PM, Trigo RM, Barriopedro D et al (2017) Responses of European precipitation distributions and regimes to different blocking locations. Clim Dyn 48(3–4):1141–1160. https://doi.org/10.1007/s00382-016-3132-5

Spellman G (2017) An assessment of the Jenkinson and Collison synoptic classification to a continental mid-latitude location. Theor Appl Climatol. https://doi.org/10.1007/s00704-015-1711-8

Stammerjohn SE, Martinson DG, Smith RC, et al (2008) Trends in antarctic annual sea ice retreat and advance and their relation to el niño-southern oscillation and southern annular mode variability. J Geophys Res: Oceans 113(C3). https://doi.org/10.1029/2007JC004269, https://agupubs.onlinelibrary.wiley.com/doi/abs/10.1029/2007JC004269

Sterl A (2004) On the (In)homogeneity of reanalysis products. J Clim 17(19):3866–3873 10.1175/1520-0442(2004)017<3866:OTIORP>2.0.CO;2, url: journals.ametsoc.org/view/journals/clim/17/19/1520-0442_2004_017_3866_otiorp_2.0.co_2.xml,

Stryhal J, Huth R (2017) Classifications of winter Euro–Atlantic circulation patterns: an intercomparison of five atmospheric reanalyses. J Clim 30(19):7847–7861. https://doi.org/10.1175/JCLI-D-17-0059.1

Taylor KE, Stouffer RJ, Meehl GA (2012) An overview of cmip5 and the experiment design. Bull Am Meteorol Soc 93(4):485–498. https://doi.org/10.1175/BAMS-D-11-00094.1

Thompson D, Wallace J (2000) Annular modes in the extratropical circulation. Part I: month-to-month variability. J Clim 13:1000–1016. https://doi.org/10.1175/1520-0442(2000)01360;1000:amitec62;2.0.co;2

Thompson D, Wallace J, Hegerl G (2000) Annular modes in the extratropical circulation. Part II: trends. J Clim 13:1018–1036. https://doi.org/10.1175/1520-0442(2000)013<1018:AMITEC>2.0.CO;2

Trenberth KE (1997) The definition of el niño. Bull Am Meteorol Soc 78(12):2771–2778

Trigo RM, DaCamara CC (2000) Circulation weather types and their influence on the precipitation regime in Portugal. Int J Climatol. https://doi.org/10.1002/1097-0088(20001115)20:13%3C1559::AID-JOC555%3E3.0.CO;2-5

Wang Y, Sun X (2020) Weather type classification and its relation to precipitation over southeastern China. Int J Climatol. https://doi.org/10.1002/joc.6747

Wang N, Zhu L, Yang H et al (2017) Classification of synoptic circulation patterns for Fog in the Urumqi Airport. Atmos Clim Sci. https://doi.org/10.4236/acs.2017.73026

Wu J, Li C, Ma Z et al (2020) Influence of meteorological conditions on ozone pollution at Shangdianzi station based on weather classification. Huanjing Kexue 41:4864–4873. https://doi.org/10.13227/j.hjkx.202003307